The Universe at Low Radio Frequencies
IAU Symposium, Vol. 199, 2002
A. Pramesh Rao, G. Swarup and Gopal-Krishna, eds.

Solar Radio Astronomy at Low Frequencies

Monique Pick

DASOP, LPSH, UMR 8645 CNRS, Observatoire de Paris, Meudon, 92195, France

Abstract.

This review is concerned to study of sun at frequencies lower than 1.4 GHz. Emphasis is made on results which illustrate the topics in which GMRT could play a major role. Coordinated studies including spectral and imaging radio observations are important for research in solar physics. Joint observations between the Giant Meter Radio Telescope (GMRT) with radio instruments located in the same longitude range are encouraged. This review inludes three distinct topics: Electron beams and radio observations- Radio signatures of Coronal Mass Ejections- Radio signatures of coronal and interplanetary shocks.

1. Introduction

Most of the recent results on solar activity emerged from coordinated observations over a large spectral domain related to different techniques. Spectral and imaging radio observations with high time resolution represent particularly an important tool for these joint studies. This review is restricted to results obtained at frequencies shorter than 1.4 GHz. Emphasis is made on results of potential interest for the field of research in which GMRT could play an important role. Finally, special attention is given to the observations performed with instruments that are located at longitudes rather close to the GMRT longitude, in China. For these instruments, imaging capability of GMRT is of the major interest. This review inludes three distinct topics: Electron beams and radio observations- Radio signatures of Coronal Mass Ejections- Radio signatures of coronal and interplanetary shocks.

2. Electron Beams and Radio Observations

2.1. Propagating Effects

Type III radio events are the signature of electron beams accelerated in the corona. Electron beams propagate along open magnetic field structures and excite Langmuir waves at each level in the corona then in the interplanetary medium. Type III signatures are the result of several processes: - energy release mechanism- acceleration mechanism- electron propagation along the magnetic field lines- generation of electromagnetic waves at the fundamental or harmonic frequencies w_p or $2w_p$.

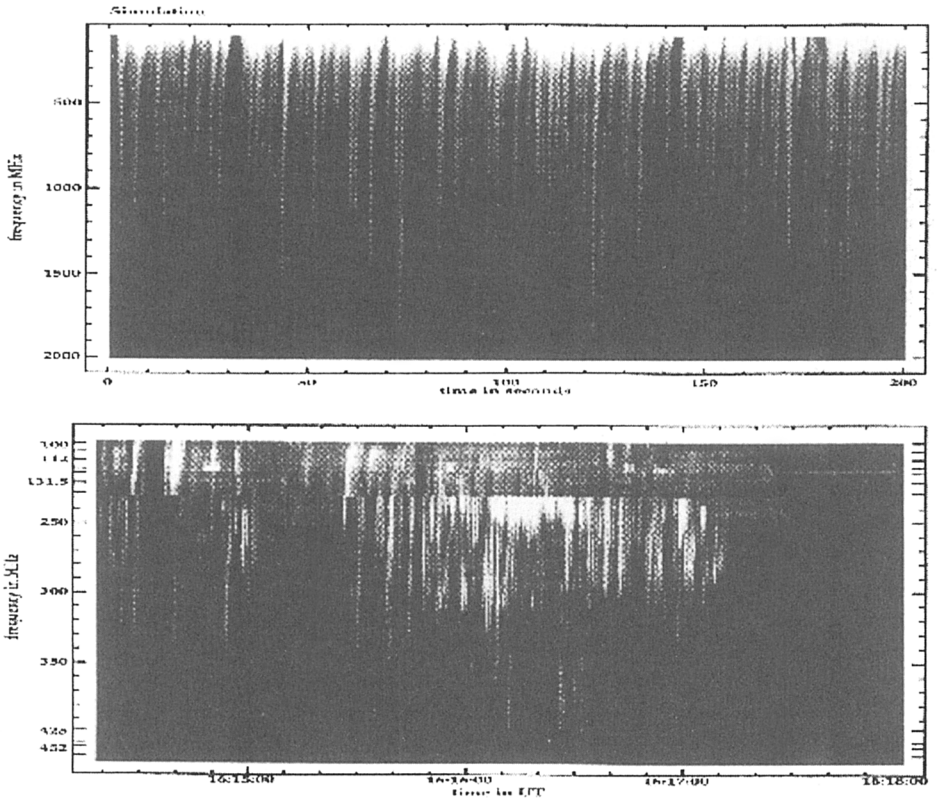

Figure 1. Upper panel: Spectrogram generated by the model (see text), with time resolution of 0.02sec and frequency resolution 55.9 MHz.Lower panel: Spectrogram of type II event on June 27 1980, observed by the ETH Zurich radio spectrometer with time resolution 0.1 sec. The two spectrograms show 200 sec duration (From Isliker et al, 1998)

https://doi.org/10.1017/S0074180900169499 Published online by Cambridge University Press

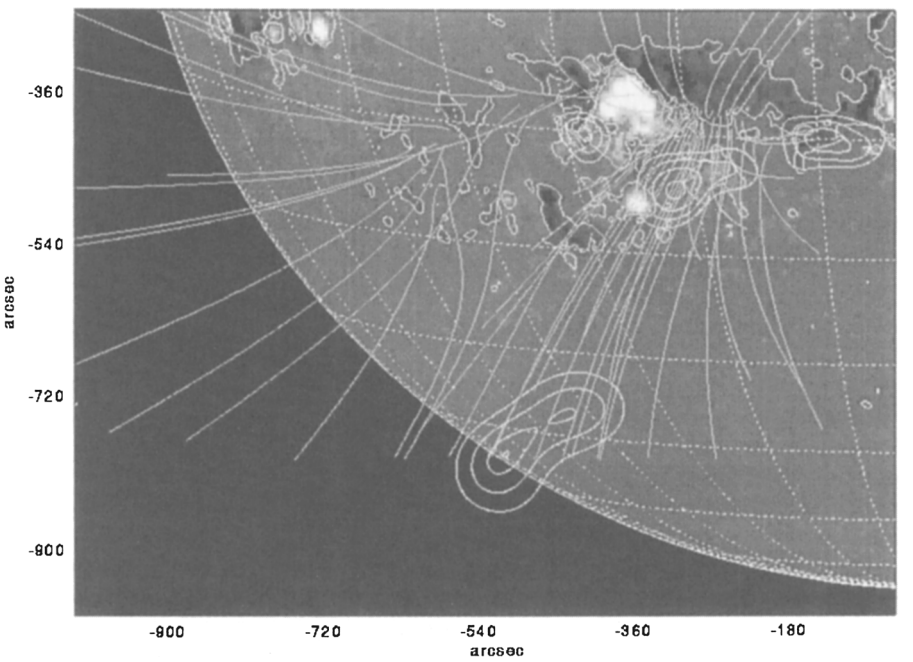

Figure 2. Photospheric magnetic field in AR 5629 from KPNO/NSO on 07/8/89, about 90 minutes after the spike event (see text). The extrapolated potential field is plotted for field lines rising to an altitude in excess of 3×10^5km. A representative VLA contour map is overlaid for each VLA frequency. The spike source at 333 MHz near the limb and the three sources around the active region are plotted (caption from Krucker et al., 1995)

https://doi.org/10.1017/S0074180900169499 Published online by Cambridge University Press

Propagating effects closely depend on the inhomegeneity of the medium. Most of the former models described in the literature considered weak spherical inhomogeneities in a stratified corona. However, in a fibrous corona, type III emission at one given observing frequency should come from a range of altitudes and it was shown that taking into account only the fibrous inhomegeneity of the corona the theory successfully simulates source evolution and dynamic spectrograms of type III bursts (Roelof and Pick, 1989). Models developed in the recent years(Vlahos et Raoult, 1995, Isliker et al., 1998) assume the following conditions: i) a strongly inhomogeneous corona constituting of a large number of fibers with a random distribution; ii) At the base of the corona, at a random time, a random number of accelerated electrons is injected along the fibers; iii) each particle distribution will develop in each fiber instability leading to Langmuir waves. Results of this simulation and comparison with observations are displayed in Figure 1. This figure shows the comparison between a spectrogram generated by the model, upper panel and a spectrogram of a type III group observed on June 27 1980 (Isliker et al., 1998)

2.2. Location of Acceleration Regions

The term spikes describes short (few tens of ms) and narrow frequency (few MHz) radio pulses. At decimeter wavelengths clouds of spikes often appear as a high frequency counterpart of type III bursts (Benz,1985).It suggests the close connection between spikes and the injection in the corona of energetic electrons. Presence of spikes may give some support to the idea of fragmentation of energy release and it was proposed that spikes and type III bursts originate from the same energy release and accelerated electron population. Spatially resolved observations of metric spikes detected at the time of type III bursts were obtained for the first time with the VLA. (Krucker et al., 1995). Figure 2 displays a VLA contour map for each VLA observing frequency at 333 MHz and 1446 MHz. These contour plots are overlaid on a photospheric magnetic field map from Kitt Peak National Observatory (KPNO). Extrapolated potential field is also reproduced for field lines rising to an altitude of 3×10^5km. The spike source is located near the limb at a projected altitude of 0.65 Rs above the photosphere, in a region of open field lines. At 21 cm, a thermal source is observed at the foot point of the field lines which brightens 40s after the spikes. The authors concluded that these observations agree with an interpretation in which metric spikes are the signature of an energy release region at high altitude, while upwards propagating electrons produce type III bursts and downward moving electrons are responsible for 21 cm thermal emissions. Yohkoh observations of the source regions of spikes confirmed recently the validity of this model(Krucker et al, 1997).

We remark that conclusions presented in Sections 2.1 and 2.2 are still based on data analysis of a few individual events and are qualitative. Combined observational effort with instruments having together high time, frequency and spatial resolutions could be encouraged. For example, spectral observations of rapid variations of solar radio emissions that are now obtained with the radiospectrograph of Beijing Astronomical Observatory could be combined in the near future with spatial observations obtained with the GMRT. Temporal resolution of this instrument which depends on the frequency is 50ms in the frequency

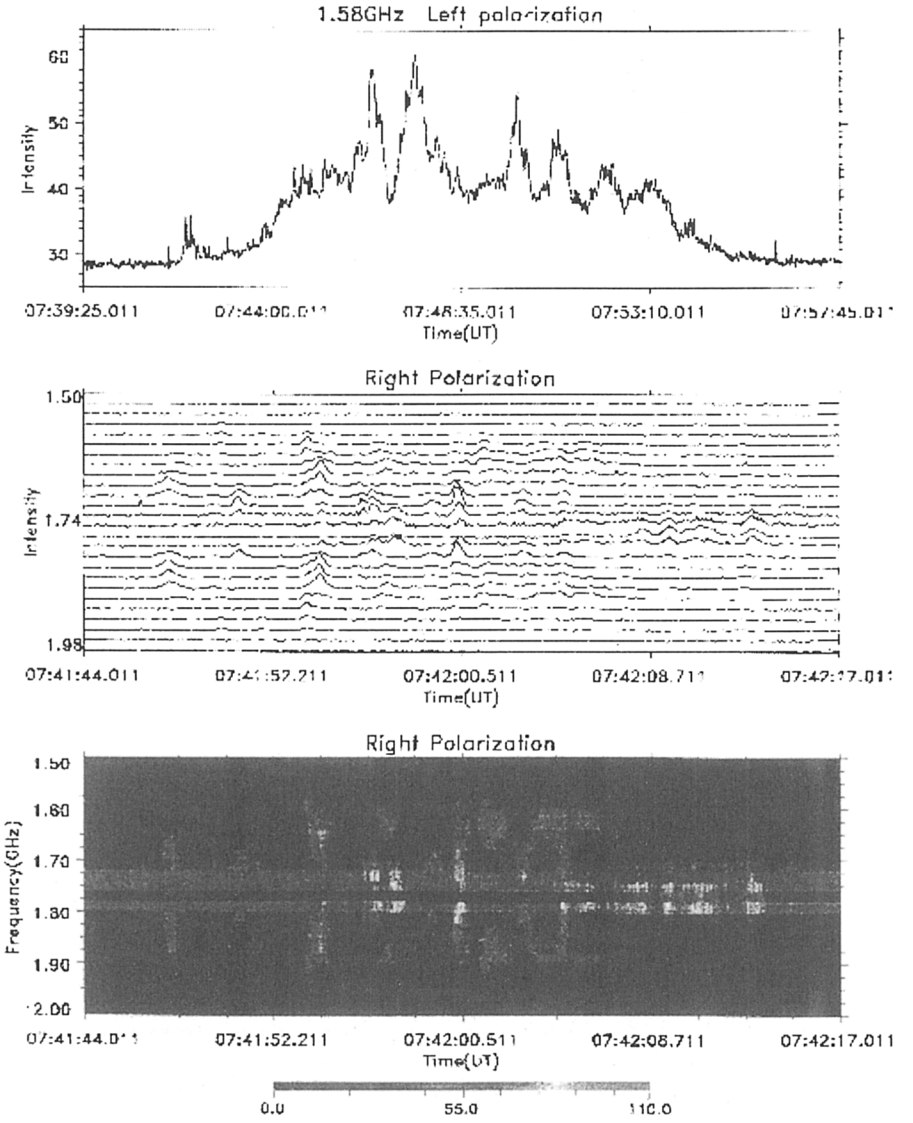

Figure 3. Radio bursts observed by the broad band spectrometer of the Beijing Astronomical Observatory. This figure displays radio emission observed in one frequency range of this instrument. The typical time resolution of the 1.-2 GHz frequency range is 50ms.(Courtoisy of Dr Yihua Yan)

https://doi.org/10.1017/S0074180900169499 Published online by Cambridge University Press

range 1.0-2.0 GHz. An example of observations performed with this instrument is shown in Figure 3. This figure shows that around 1.7-1.8 GHz, bursts with both negative and positive frequency drifts are detected. They are interpretated as forward and downward electron beams escaping from the acceleration region in agreement with Stahli and Benz (1987)

3. Radio Signatures of Coronal Mass Ejections

Coronal Mass Ejections (CMEs are the most spectacular coronal events observed by white light coronagraphs. With the launch of SOHO mission, the LASCO coronagraphs have provided for the first time a large field of view from 1.1 to 30 solar radii (Bruckner et al., 1995). At distances outside SOHO range, the radio scintillation measurement can provide kinematical properties of the propagating CMEs (Manoharan et al., 2000). There exist different classes of CMEs. Many CMEs are associated with active prominence eruptions and other ones with flares. The most recent results using radio techniques concern tflare/CME events. For these events, accelerated electron beams which propagate along magnetic field lines excite through plasma mechanism radio bursts which are recognized as accurate tracers of the coronal magnetic field. This is illustrated in Figures 4 which displays the evolution of the November 6 1997 CME event (Maia et al., 1999). A sketch of the successive coronal structures involved in the development of this CME is represented in the lower panel. The upper panel displays composite images of one magnetogram image provided by MDI aboard SOHO (Scherrer et al., 1995) with the two LASCO C1 and C2 images. The C1 Fe X images show two distinct loops. These loops, labeled II on the sketch expand rapidly and the next image displays the CMEin white light in C2 field of view 12 minutes later. The CME propagates with a constant projected speed of about 1900 km/s.

The progression of the CME is observed by the Nancay Radioheliograph every second. The initial instability which is revealed in the radio data by occurrence of very short bursts is located in a small volume at the edge of the flaring region. Then within the few next seconds, the radio emission reveals the existence of two successive expanding loops in the southern hemisphere. These loops labeled I on the sketch are also detected in the field of view of C2 later on. The speed is approximately 3000 km/s. The images displayed in the lower panel show the evolution in complexity of the radio sources. This evolution corresponds to a succession of loop interactions progressing from the southern to the northern hemisphere and which lead to the opening of the magnetic field over a latitude range of 100 °. The sites of radio emission are located in regions of interaction of two adjacent loop structures and appear successively in positions labeled A, B-B′, C on the sketch. The figure shows also that an excellent agreement is found between the extent in latitude of the CME seen in radio and white light respectively. The time interval between the initial instability and the full development of the CME is about 4 minutes. In conclusion, there is a close spatial and temporal association between the CME development seen respectively in white light and in radio; the full development of the CMEs is reached within the first few minutes. The CMEs propagate with a nearly constant velocity. It is pointed out that the opening of the magnetic field over a

large volume allows the fast transport of coronal particle in both latitude and longitude from the flare site.

Halo events correspond to CMEs that originate above the solar disk and which are directed towards or away from the Earth (Howard et al., 1982). This is now well established that they are ends of view of three dimensional structures. These CMEs originate on the solar disk and quickly expand to a projected size larger than the occulting disk of coronagraphs. Figure 5, left side, displays one image seen in the external LASCO C3 coronagraph of the halo event observed on May 02 1998. This image also reveals the "snow rain" of energetic particles hitting on the CCD detector and caused by the same flare/CME event. Such Earth directed events are of particular interest for their geomagnetic and space weather effects. Coronagraph instruments observe such events when they have reached high altitudes in the corona. They cannot distinguish between forward and backward events. XUV and radio imaging instruments observe the corona above the solar disk and radio observations can probe a CME at various altitudes depending on the observing frequency. Disk observations, as displayed in Figure 5, right side, show for these events a similar evolution to those observed above the solar limb: several large scale magnetic arches are involved in the development of CMEs and interact together (Pick et al., 1999).

4. Coronal and Interplanetary Shocks: Type II Bursts

Type II radio bursts are slow drifting frequency emissions observed on radio spectra. They are attributed to electrons accelerated by shocks which excite Langmuir waves that lead to electromagnetic emissions at the local plasma frequency and/or at its harmonics. The observed frequency drift results of the decrease in the plasma density with increasing distance of the sun and the frequency drift rate is directly related to the speed of the shock. They are usually observed below 400 MHz (Zlobec et al., 1993). Metric type II bursts are believed to be generated by flare associated coronal shocks whereas interplanetary (kilometric) shocks are generated by interplanetary shocks driven by coronal mass ejections (e g.Cane et al., 1987, Reiner and Kaiser, 1999). Origin of coronal shocks is not yet understood. Comparison between radio images and coronagraph data shows clear evidence that most of metric type II bursts are indeed not associated with CME shocks (e.g; Pick, 1999) High temperature fast short lived X- ray ejecta issued from the flare region have been proposed as possible candidates to drive the shock (Gopalswamy et al., 1998, Klein et al., 1999). In addition, although still based on the data analysis of a few events, recent observations suggest a spatial and temporal association between metric type II bursts and transient EUV waves (Gopalswamy et al., 2000). These transient EUV waves were detected at 195 A with the Ultraviolet Imaging Telescope (EIT) of the SOHO spacecraft. (Thomson et al., 1998). An example of this association between metric type II bursts and EIT waves is shown in Figure 6. This figure shows the contour map of the type II burst at 164 MHz superposed on the EIT image taken at the same time. The centroid of the type II burst coincides with the brightest portion of the EIT waves. .

On the other hand, evidence for the existence of metric radio bursts spatially associated with the front edge of CMEs have been recently observed. (Maia

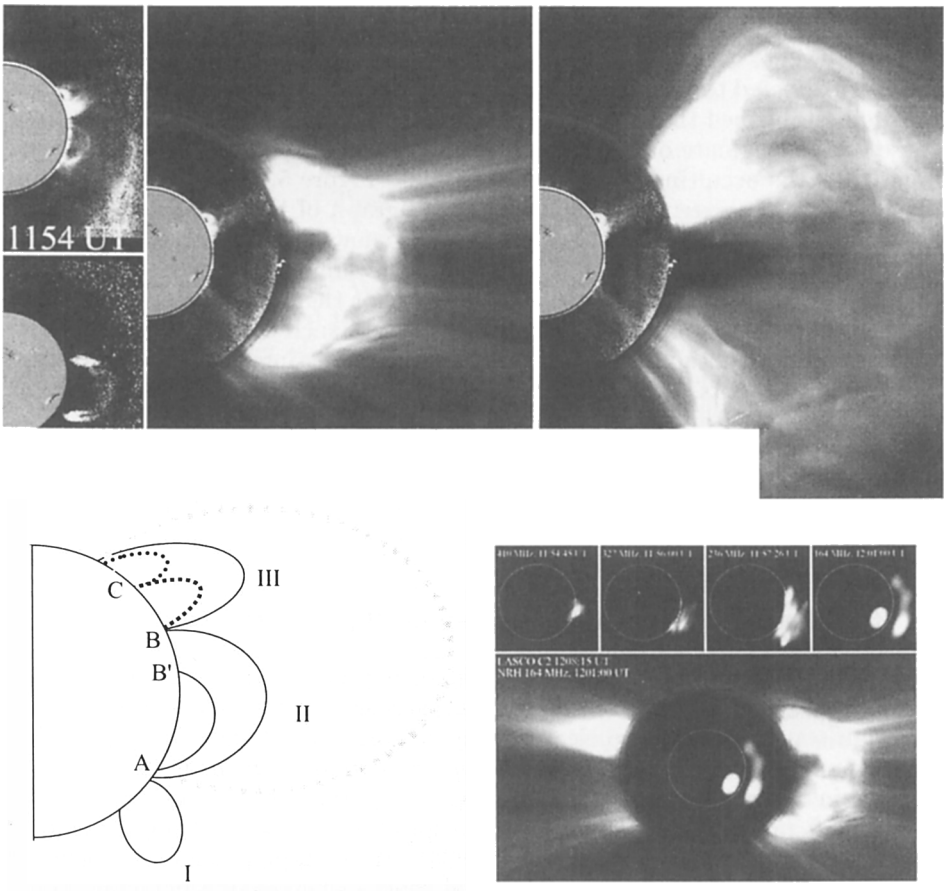

Figure 4. November 6 1997 event.Upper panel: Composite images of one magnetogram image provided by MDI aboard SOHO (Scherrer et al., 1995) with LASCO C1 Fe X and C2 images (see text). The C1 images show the progression of a loop labeled II in the sketch displayed on the lower panel. Stable loops labeled III are also observed at the north edge.The C2 image, on the right side shows the progression of the CME. Lower panel, right: The radio images show the evolution in complexity of the source; the composite image of one C2 image with one radio image at 164 MHz shows that there is a good correspondence between the extend in latitude of the CME seen by C2 and the radio-heliograph.The sketch. represents the successive coronal loops involved in the development of the CME. A, B-B′ and C are the site of radio emitting sources. They correspond to regions where two adjacent loops are interacting (From Maia et al., 1999).

https://doi.org/10.1017/S0074180900169499 Published online by Cambridge University Press

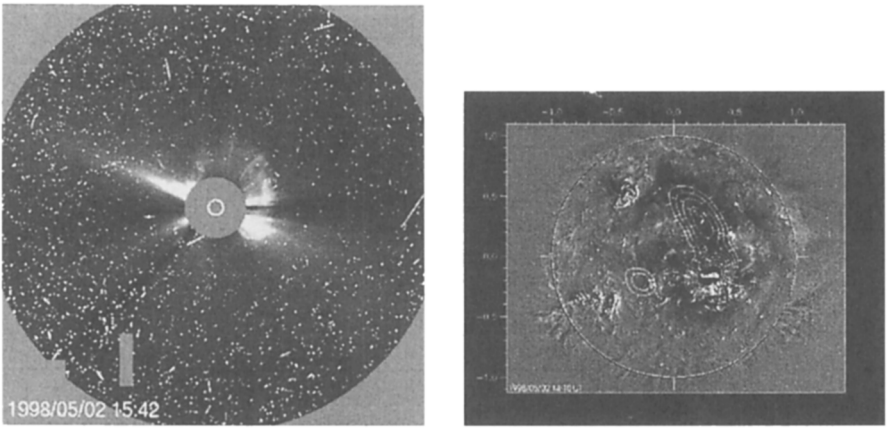

Figure 5. The May 02 1998 Halo CME event. Left panel: Halo CME in LASCO C3. Right panel:Contours of the radio source at 164 MHz have been superposed on one image of the EIT telescope (see text); a large coronal arcade overlies the dimming region which reveals one aspect of the CME development seen on the disk

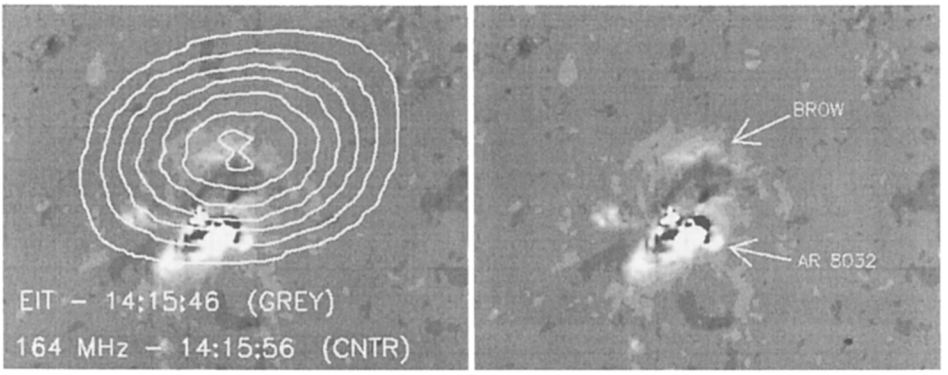

Figure 6. Superposition of 164 MHz type II burst contours on an EIT difference image obtained by subtracting the 13:41 UT image a preevent image. The EIT wave can be clearly seen to the north of AR 8032. North is to the top and east to the left(From Gopalswamy et al., 2000)

https://doi.org/10.1017/S0074180900169499 Published online by Cambridge University Press

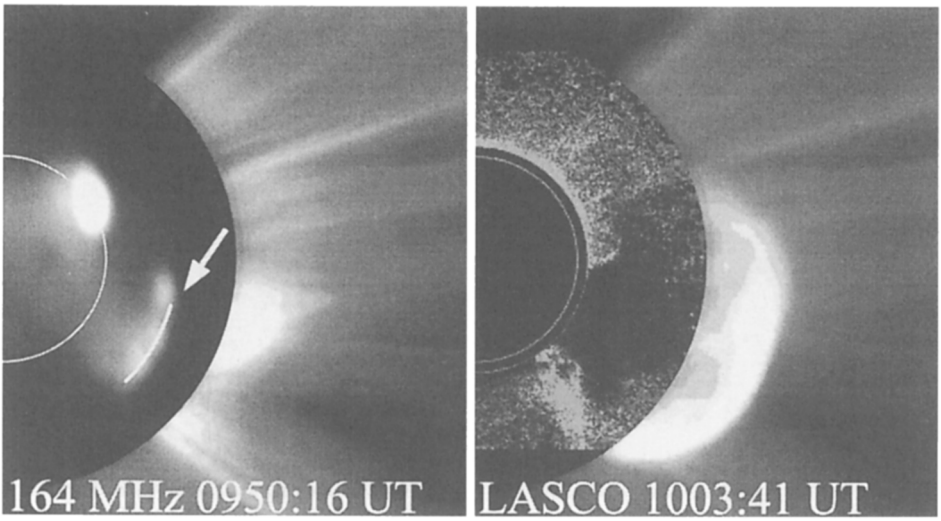

Figure 7. The April 20, 1998 event. Leading edge of the CME as seen by the NRH (left) and later by LASCO C2 (right). The position of the leading edge observed by C2 has been extrapolated back at the time of the NRH observation and corresponds to the thick line reported on the figure (left) (From Maia et al., 2000)

et al., 2000). They look like weak type II bursts most often not detected on spectrograms. Figure 7 displays the progression of an event observed on April 20, 1998. The position of the radio source coincides precisely with the leading edge of the CME.This emission is the counterpart of interplanetary type II bursts observed in the interplanetary medium.

5. Concluding Remarks

It has been shown that radio imaging of the sun is of great interest for the understanding of the dynamical behaviour of the corona.However, our knowledge is still incomplete and qualitative on many points such as evidence for magnetic field reconnection in the corona and origin of particle acceleration. For many purposes, the high spatial resolution of the GMRT open the way to very new research projects. This is expected that combined studies involving GMRT and in the future STEREO mission or possibly the solar probe will be encouraged.

Acknowledgments. I am grateful to P. K. Manoharan for helpful comments.

References

Benz A. O. 1985, Solar Phys., 96, 357
Brueckner, G. E. & al. 1995, Solar Phys., 162, 357

Cane, H. V., Sheeley, Jr N. R. & Howard R. A., 1987, J. Geophys. Res., 92, 9869-9874

Howard, R. A., Michels, D. J., Sheeley, N. R., Jr. & Koomen, M. J., 1982, ApJ, 263, L101-L104

Gopalswamy, N. & al. 1998, J. Geophys. Res., 103, A10, 307

Gopalswamy, N., Kaiser, M. L., Sato, J. & Pick, M. 2000, in High Energy Solar Physics: Anticipating HESSi ASP Conference Series, in press, R. Ramaty and N. Mandzhavidze, eds.

Isliker, Vlahos, L., Benz, A., & Raoult, A. 1998, Astron. Astrophys,336, 371

Klein, K. L. & al. 1999, Astron. Astrophys., 346, L 53

Krucker, S., Aschwanden, M.J., Bastian T.S. & Benz A. 1995, Astron. Astrophys.,302, 551-563

Krucker & al., 1997

Maia., D., Vourlidas, A., Pick, M. & Howard, R 2000, ApJ L, 528, L49-51

Maia, D., Vourlidas, A., Pick, M. & Howard, R., 1999, J. Geophys. Res., Vol 104 A6 12507-12513

Manoharan, P. K.& al. 1996, ApJ L, 468, L 73

Pick, M. & al., 1999, Solar Wind 9 Conference, Ed. S. Habbal,649

Reiner, M. J. & Kaiser M. L. 1999, J. Geophys. Res., 104, 16979

Roelof, E. C. & Pick, M. 1989, Astron. Astrophys., 210, 417

Scherrer, P. H. & 1995, Sol. Phys., 162, 129

Thomson, B. J. & al., 1998, Geophys. Res. Let., 25, 14

Stahli, M. & Benz, A. O. 1987, Astron. Astrophys., 175, 271

Vlahos, L. & Raoult, A. 1995, Astron. Astrophys., 139, 263

Zlobec, P. Messerotti, M., Karlicky, M. & Urbarz, H., 1993, Solar Phys., 144, 373